Eur. Phys. J. D **17**, 67–74 (2001)

THE EUROPEAN PHYSICAL JOURNAL D

EDP Sciences

An analytical study of a periodically driven laser with a saturable absorber

T.W. Carr[1,a] and T. Erneux[2,b]

[1] Department of Mathematics, Southern Methodist University, Dallas, TX 75275-0156, USA
[2] Université Libre de Bruxelles, Optique Nonlinéaire Théorique, Campus Plaine, C.P. 231, 1050 Bruxelles, Belgium

Received 10 March 2001

Abstract. We consider the rate equations for a laser with an intracavity saturable absorber and subject to a periodically modulated pump. By deriving simplified equations for a map valid for strongly pulsating regimes, analytical conditions are determined that specify the properties of both frequency-locked and unlocked behaviors. As the strength of the modulation is increased, quasiperiodic and period-doubling bifurcations are predicted. However, only the transition from locking to non-locking through a quasiperiodic bifurcation is possible for realistic values of the parameters. Our results are consistent with previous numerical and experimental studies of modulated lasers with a saturable absorber.

PACS. 42.65.Sf Dynamics of nonlinear optical systems; optical instabilities, optical chaos and complexity, and optical spatio-temporal dynamics – 42.60.Fc Modulation, tuning, and mode locking – 42.60.Gd Q-switching

1 Introduction

Lasers with an intracavity saturable absorber (LSA) have long been used to generate high-intensity pulses (see [1–4] for background and historical references). The absorber acts to limit the light output and hence prevent depletion of the active media. However, a threshold is reached such that the absorber becomes transparent and allows a rapid depletion of the now very strong population inversion and the emission of a pulse. The effect is similar to "Q-switching" the laser-cavity losses and hence the LSA is said to exhibit a "passive Q-switch" (PQS) behavior. The PQS output is of practical interest for applications that require extremely short (< 1 ns) high-peak-power (> 10 kW) pulses of light. The short pulse widths are useful for high-precision optical ranging with applications in automated production. The high peak output intensities are needed for efficient nonlinear frequency generation or ionization of materials, with applications in micro-surgery and ionization spectroscopy. Combined theoretical and experimental studies of PQS first considered gas lasers [5,6] and then concentrated on microchip solid state lasers and semiconductor lasers. Microchip lasers are small, easy to manipulate and offer high performances for the pulse width and/or peak-power [7,8]. Self-pulsing semiconductor lasers exhibit a high repetition rate which ranges from hundreds of megahertz to a few gigaHertz [9, 10]. They are interesting for telecommunication and for optical data storage using compact disc (CD) or digital versatile disc (DVD) systems [11–17].

Frequency jitter (stochastic variations in the frequency) in oscillating systems such as the LSA can be reduced by frequency-locking the system to an external drive source with more stable periodic output [18–20]; in lasers, this is often referred to as "linewidth narrowing". The goal of achieving linewidth narrowing has motivated a number of studies of the "modulated LSA" (LMSA) [12,18–22]. In these works, the frequency-locking characteristics and the unlocked behavior of the LMSA have been investigated both numerically and experimentally. The unlocked behavior includes quasiperiodic output and chaos. Practically, we would like good locking properties for stable, tunable laser outputs. The interest of periodically modulated LSA for applications, the experimental observation of complex dynamics, and the numerical simulation of these phenomena using rate-equations, motivate analytical studies.

The main objective of this paper is to derive simple conditions that describe the locking region of the LMSA as a function of the modulation amplitude and frequency. These conditions show a variety a locking possibilities, emphasize the role of certain parameters, and predict bifurcation points possibly leading to complex (chaotic) dynamics. The formulation of the LSA dimensionless equations depends on the type of laser but is documented in the literature. See, for example, references [5,6] for CO_2 lasers, reference [24] for self-pulsating diode lasers, and reference [30] for microchip solid state lasers. The LMSA two-level atoms rate equations for the intensity of the laser

[a] e-mail: tcarr@mail.smu.edu
[b] e-mail: terneux@ulb.ac.be

field I and the population inversions of the active and passive regions, D_1 and D_2, are given by

$$\begin{aligned}\frac{\mathrm{d}I}{\mathrm{d}t} &= [D_1 + D_2 - 1]I,\\ \frac{\mathrm{d}D_1}{\mathrm{d}t} &= \gamma_1[A_1(1+\delta\cos(\omega t)) - (1+I)D_1]\\ \frac{\mathrm{d}D_2}{\mathrm{d}t} &= \gamma_2[A_2 - (1+aI)D_2]. \end{aligned} \quad (1)$$

The parameters γ_1 and γ_2 are the decay rates of D_1 and D_2 normalized by the cavity decay rate, respectively. $A_2 < 0$ is defined as the absorber pump parameter and a describes the relative saturability of the absorber with respect to the active media. The first term in the equation for D_1 models a periodically modulated pump parameter where A_1, δ and ω represent its averaged value, its modulation amplitude, and its normalized modulation frequency, respectively. Typical values of the laser parameters are documented in [5,6] for CO_2 lasers, in [23] for microchip solid state lasers, and in [24] for semiconductor lasers. The range of values of these parameters may depend on the type of laser but they all exhibit small values of γ_1 and γ_2 (10^{-5} to 10^{-3}). The strongly pulsating behavior of PQS is directly related to these small values of γ_1 and γ_2 [29]. For self-pulsing semiconductor lasers, (1) needs to supplemented by additional terms modeling nonlinear gain saturation, nonlinear damping of D_1 and D_2, and cross-diffusion of the carriers between active and passive regions. However, none of these additional effects are responsible for the generation of PQS [24]. Self-pulsation appears through a bifurcation mechanism which we briefly review. If $\delta = 0$, the domain of pulsating intensities is bounded by either the laser first threshold and a Hopf bifurcation point or by two Hopf bifurcation points. In the latter case, the low intensity Hopf bifurcation point is located very close to the laser first threshold and the leading approximation of the domain of self-pulsation is mathematically the same for both cases in the limit of small values of γ_1 and γ_2. In terms of A_1, the domain of self-pulsation is approximately given by

$$A_{\mathrm{th}} < A_1 < A_{\mathrm{H}} \quad (2)$$

where $A_{\mathrm{th}} \equiv 1 - A_2$ is defined as the laser first threshold and A_{H} corresponds to a high intensity Hopf bifurcation point; the expression for A_{H} is not needed for our analysis. The laser intensity oscillations are strongly pulsating near A_{th} and exhibits long interpulse periods. They progressively become smoother as we increase A_1 and approach A_{H}.

Equation (1) simplifies if we adiabatically ($\gamma_2 \gg \gamma_1$) eliminate D_2. From equation (1), we then obtain the following two equations

$$\begin{aligned}\frac{\mathrm{d}I}{\mathrm{d}t} &= \left[D + \frac{A_2}{1+aI} - 1\right] I,\\ \frac{\mathrm{d}D}{\mathrm{d}t} &= \gamma[A(1+\delta\cos(\omega t)) - (1+I)D] \end{aligned} \quad (3)$$

where $D = D_1$, $\gamma = \gamma_1$ and $A = A_1$. Equation (3) is studied in detail in [22] and has been shown to possess many dynamical features of equation (1). An adiabatic elimination of D_2 is also proposed in [19] from the four-level atoms rate equations. We have studied the PQS regimes of both equation (1) and equation (3) and did not find qualitative differences for the PQS locking conditions. In this paper, we concentrate on the pulsating solutions of equation (3) appearing for γ small. In this limit, the domain of pulsating intensities is given by (2) where $A_{\mathrm{th}} = 1 - A_2$ and $A_{\mathrm{H}} \approx [-A_2/(a\gamma)]^{1/2}$.

Lauterborn and Eick [22] have shown that the LSA equations can be written as a perturbed Hamiltonian. This suggests the possibility of using methods such as averaging or subharmonic-Melnikov theory [26,27] to analyze the LMSA. However, the dissipation is not uniformly small over the complete period of the orbit, and this prevents the use of the averaging type methods.

Our analysis will make explicit use of the pulsating nature of PQS where the high-intensity pulses are followed by a long time during which the intensity is close to zero. By using the method of matched asymptotic expansions [28], we obtain asymptotic approximations to the dynamics in each regime. This enables us to construct a map for the amplitude and period from one pulse to the next. Fixed points of the map then correspond to frequency-locked solutions of (3).

The derivation of the map is given in Section 2 and the analysis of its fixed points is described in Section 3. In Section 4, we discuss the physical implications of our results.

2 A map describing PQS with modulation

To analyze the LSA in the regime of PQS, we take advantage of the fact that the high-intensity pulses are followed by a period during which the intensity is nearly zero. We will use different asymptotic approximations for (3) to analyze each regime in the spirit of "boundary-layer" analysis [28]. This approach has been used to analyze the period and maximum amplitude of the free PQS in [29,30]. Our problem is however more complicated because we consider a time-periodic pump. For the simpler problem of a modulated class-B laser, this has been done in [31,32]. The results of the analysis are given by equations (8, 9) for the "MPQS-map". This map determines the time T_{n+1} and inversion D_{n+1} of the next pulse given T_n and D_n of the present pulse. Increasing n allows us to determine how the period of the pulses and the inversion (from which we can determine the intensity) evolve in time. Since the mathematical analysis is similar to the one described in [29], we only emphasize the analytical differences.

2.1 The interpulse regime

We first investigate the interpulse regime during which $I \ll 1$ and D increases from $D(T_0)$ to $D(T_1)$ (Fig. 1). In (3), we let $T \equiv \gamma t$ and assume $I \ll 1$. The equation for

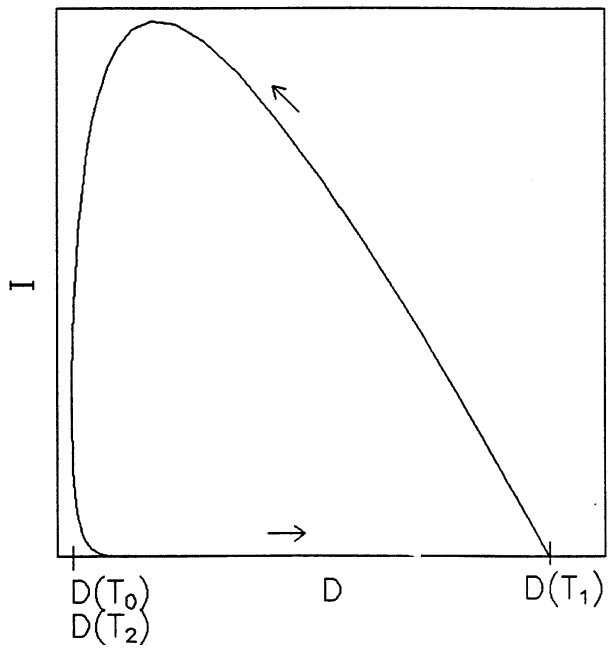

Fig. 1. PQS limit-cycle in the phase plane (I, D). A complete orbit starts at $D(T_0)$ and finishes at $D(T_2)$. It consists of the interpulse regime where D slowly increases from $D(T_0)$ to $D(T_1)$ ($I \ll 1$) followed by the pulse regime where $D(T_1)$ quickly changes to $D(T_2)$ ($I \gg 1$).

D is then linear, in first approximation, and integrating from T_0 to T, we find

$$D(T) = A(1 + R\cos(\Omega T + \phi)) + [D(T_0) - A(1 + R\cos(\Omega T_0 + \phi))]\mathrm{e}^{-(T-T_0)} \quad (4)$$

where $\Omega \equiv \omega/\gamma$, $R \equiv \delta(1 + \Omega^2)^{-1/2}$ and ϕ satisfies the equation $\tan(\phi) = -\Omega$. We next substitute the expression (4) into the right hand side of the equation for I, assume $I \ll 1$ again, integrate and obtain

$$\gamma \ln\left[\frac{I(T)}{I(T_0)}\right] = (A - A_{\mathrm{th}})(T - T_0) + [D(T_0) - A(1 + R\cos(\Omega T_0 + \phi))]\left(1 - \mathrm{e}^{-(T-T_0)}\right) + \frac{AR}{\Omega}\left(\sin(\Omega T + \phi) - \sin(\Omega T_0 + \phi)\right) \quad (5)$$

where $A_{\mathrm{th}} = 1 - A_2$. During the interpulse regime, the right hand side of equation (5) is negative and $I(T)$ remains exponentially small. This regime ends at time $T = T_1$ when $I(T_1) = I(T_0)$. Using (5), we obtain the following implicit equation for T_1

$$\begin{bmatrix} (A - A_{\mathrm{th}})(T_1 - T_0) \\ +[D(T_0) - A(1 + R\cos(\Omega T_0 + \phi))](1 - \mathrm{e}^{-(T_1 - T_0)}) \\ +\frac{AR}{\Omega}(\sin(\Omega T_1 + \phi) - \sin(\Omega T_0 + \phi)) \end{bmatrix} = 0. \quad (6)$$

2.2 The pulse regime

The slow interpulse regime is followed by a quick and intense pulse. However, the modulations do not perturb the pulse in first approximation. Consequently, our analysis will be identical to the analysis of the free PQS pulse [29]. Integrating in the phase plane leads to an equation describing the quick change of D from $D(T_1)$ to $D(T_2)$ (Fig. 1). This equation is given by

$$\ln\left[\frac{D(T_2)}{D(T_1)}\right] - (D(T_2) - D(T_1)) = 0. \quad (7)$$

2.3 The equations for a map

Equations (4, 6, 7) are used to construct a map describing the PQS dynamics in the form $(T_n, D_n) \mapsto (T_{n+1}, D_{n+1})$. The map iterates (T_n, D_n) defined as the time and the value of the inversion at the end of each pulse, *e.g.* $D(T_0)$, $D(T_2)$, etc., see Figure 1. Given T_0 and $D(T_0)$, we first obtain T_1 and $D(T_1)$ from equations (6, 4), respectively. The initial conditions for the next pulse are then $T_2 \approx T_1$ and $D(T_2)$ obtained from (7). This leads to the following two equations relating T_{n+1}, T_n, D_{n+1} and D_n

$$T_{n+1} = T_n + P(T_n, D_n), \quad (8)$$

$$\ln\left[\frac{D_{n+1}}{G(T_n, D_n)}\right] - [D_{n+1} - G(T_n, D_n)] = 0. \quad (9)$$

P is the period of one complete orbit and $G \equiv D(T_1)$. They satisfy transcendental equations given by (6) and by (4) evaluated at $T = T_1$:

$$0 = (A - A_{\mathrm{th}})P + [D_n - A(1 + R\cos(\Omega T_n + \phi))](1 - \mathrm{e}^{-P}) + \frac{AR}{\Omega}[\sin(\Omega(T_n + P) + \phi) - \sin(\Omega T_n + \phi)], \quad (10)$$

$$G = A[1 + R\cos(\Omega(T_n + P) + \phi)] + [D_n - A(1 + R\cos(\Omega T_n + \phi))]\mathrm{e}^{-P}. \quad (11)$$

The equations for the map look complicated but considerable progress has been achieved. Pulsating periodic solutions of the LMSA problem now correspond to fixed points of these equations. Furthermore, these equations considerably simplify for the fixed points as we shall demonstrate in the next section. Note that parameter a do not appear in the leading equations for the map. Consequently, the map ignores the upper Hopf bifurcation point and is essentially valid near the laser threshold.

3 Fixed points

We look for fixed points of the form

$$T_n = nT_{\mathrm{f}} + T_0 \text{ and } D_n = D_{\mathrm{f}}. \quad (12)$$

From (8) we find the condition

$$T_{\mathrm{f}} = P(nT_{\mathrm{f}}, D_{\mathrm{f}}). \quad (13)$$

But for frequency locking, the period P must be independent of n in equation (10), which implies the condition

$$T_{\rm f} = P = \frac{2\pi m}{\Omega} \cdot \tag{14}$$

Thus, $T_{\rm f}$ is determined by the forcing frequency Ω. Note that with (14), equation (10) for $P = T_{\rm f}$ simplifies as

$$0 = \lambda T_{\rm f} + [D_{\rm f} - A(1 + R\cos\Phi)](1 - \exp(-T_{\rm f})), \tag{15}$$

where $\lambda \equiv A - A_{\rm th}$ and $\Phi \equiv \Omega T_0 + \phi$. Using (15), equation (11) also simplifies and gives

$$G_{\rm f} = D_{\rm f} + \lambda T_{\rm f}. \tag{16}$$

In order to find $D_{\rm f}$, we substitute (16) into equation (9) and solve for D. We find

$$D_{\rm f} = \frac{\lambda T_{\rm f}}{{\rm e}^{\lambda T_{\rm f}} - 1} \cdot \tag{17}$$

Finally, $D_{\rm f}$ is introduced into equation (15) and solving for $R\cos(\Phi)$, we determine a relation between the forcing amplitude $\delta = R(1 + \Omega^2)^{1/2}$ and period $T_{\rm f}$ given by

$$\delta\cos(\Phi) = \delta_{\rm SN} \equiv \left[1 + \left(\frac{2\pi m}{T_{\rm f}}\right)^2\right]^{1/2} \times \left[-1 + \frac{\lambda T_{\rm f}}{A}\left(\frac{{\rm e}^{\lambda T_{\rm f}} - {\rm e}^{-T_{\rm f}}}{(1 - {\rm e}^{-T_{\rm f}})({\rm e}^{\lambda T_{\rm f}} - 1)}\right)\right] \cdot \tag{18}$$

Equations (14, 18) define fixed points of the map, *i.e.*, a possible solution for the unknown phase Φ. If $T = T_{\rm LC}$ denotes the period of the free PQS limit-cycle, $T_{\rm LC}$ satisfies equation (15) with $R = 0$. For large values of $T_{\rm f}$ and $T_{\rm LC}$ (λ fixed), equation (18) simplifies as

$$\delta\cos\Phi \simeq \frac{\lambda}{A}\left[1 + \left(\frac{2\pi m}{T_{\rm f}}\right)^2\right]^{1/2}(T_{\rm f} - T_{\rm LC}) \tag{19}$$

which we recognize as the steady Adler's equation [33,34] for steady state locking in a laser subject to injection. If the detuning $T_{\rm f} - T_{\rm LC}$ is too large or if the modulation amplitude δ is too small, equation (19) does not admit a solution and frequency-locking is not possible. The limit λ small and $T_{\rm f} = O(\lambda^{-1})$ large of equation (18) (near threshold conditions) is studied in detail in the Appendix.

There are different ways of analyzing equation (18) which we now describe.

3.1 Changing the laser limit-cycle frequency

We keep δ fixed and consider the laser operating at $\Phi = 0$. By changing $\lambda = A - A_{\rm th}$, we change $T_{\rm LC}$ defined as the natural period of the laser. In order to maintain locking, the modulation frequency then needs to be changed. From (18), we determine $T_{\rm f}$ and in Figure 2, we represent $T_{\rm f} = 2\pi m/\Omega$ as a function of λ. Note that $T_{\rm f}$ needs to be large for low values of λ because $T_{\rm LC}$ becomes large as the pump parameter comes close to threshold.

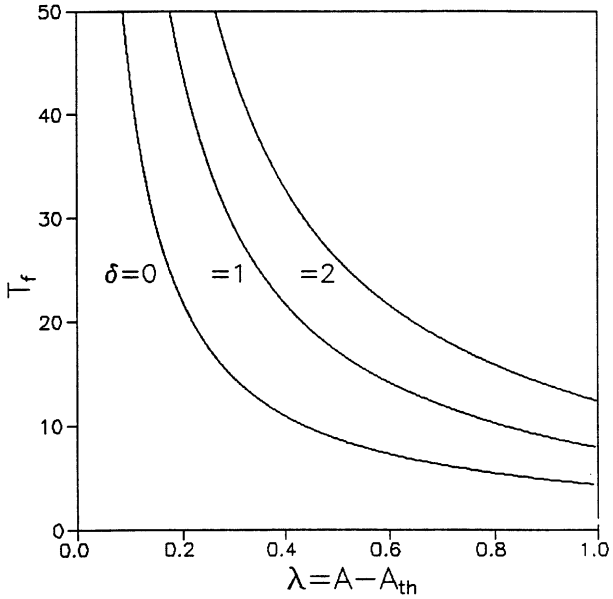

Fig. 2. For fixed δ, the period $T_{\rm f}$ as a function of $\lambda = A - A_{\rm th}$ ($A_2 = -3.4375$). When $\lambda \to 0^+$ the system approaches a homoclinic solution.

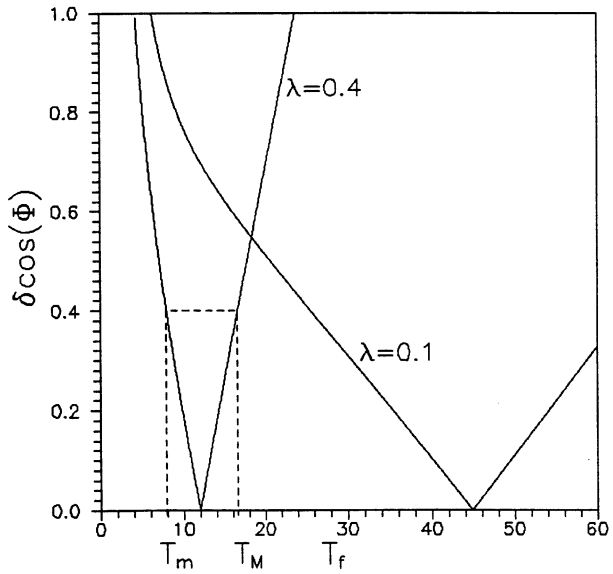

Fig. 3. Primary ($m = 1$) frequency locking region for different operating conditions (different λ). For a fixed $\delta = 0.4$, $T_{\rm f}$ is in the interval $T_{\rm f} \in [T_m, T_M]$ as Φ decreases in the interval $\Phi \in [\pi, 0]$ ($A_2 = -3.4375$).

3.2 Changing the modulation frequency

We consider all parameters fixed except for the phase Φ and the modulation frequency Ω. Locking is possible if there exists a value of $0 \leq \Phi \leq \pi$ satisfying equation (18). In Figure 3, we consider the case $m = 1$ and show the locking region for two values of λ. The possible solutions are bounded by $T_{\rm f} = T_m$ when $\Phi = \pi$ and by $T_{\rm f} = T_M$ when $\Phi = 0$. Furthermore, $T_{\rm f} = T_{\rm LC}$ when $\Phi = \pi/2$ and from this point emerges two lines. The change in the phase

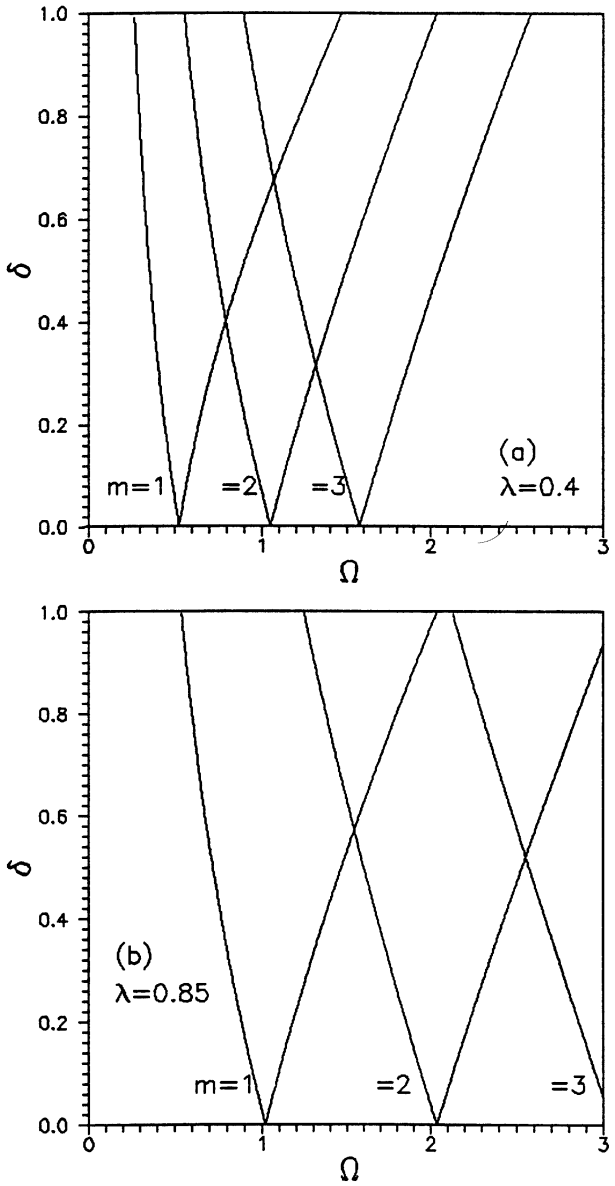

Fig. 4. Frequency-locking regions for (a) $\lambda = 0.40$ (b) $\lambda = 0.85$ and several resonances ($m = 1, 2$ and 3). Quasiperiodic behavior occurs outside the Arnold tongues.

with respect to the locking frequency Ω has been observed experimentally by Egan *et al.* [21].

In Figure 4, we show the well known "Arnold tongues" [26] corresponding to different values of m (different resonances). For $\lambda = 0.40$ (Fig. 4a) we let $T_f = 2\pi m/\Omega$, $m = 1$, 2, 3 in (18). For fixed m the curves define Ω_m and Ω_M on the left and right, respectively. Outside the Arnold tongues, the LMSA exhibits quasiperiodic behavior.

Recall from Figure 2 that the laser's natural frequency is highly tunable with λ. This greatly affects the qualitative nature of the Arnold tongues. For low values of λ, the unforced laser is in the highly pulsating regime. Here the Arnold tongues are shifted to lower frequencies, are narrower, and are more closely spaced. On the other hand, if

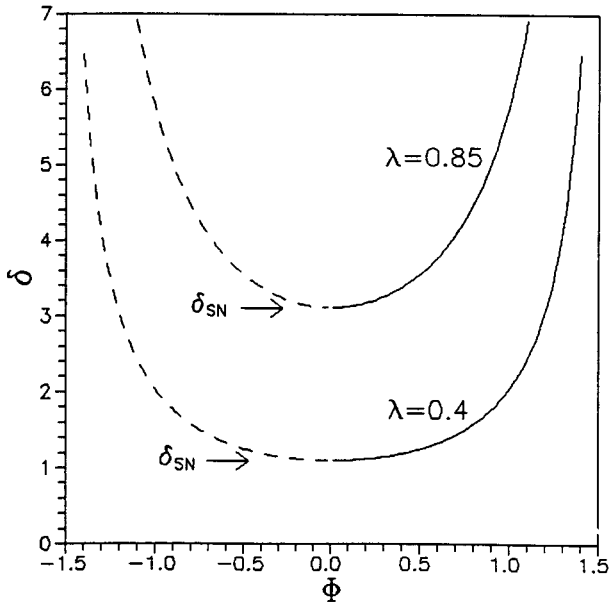

Fig. 5. For fixed λ and period $T_f = 2\pi/\Omega = 25$, frequency locking occurs at a minimum value $\delta = \delta_{SN}$ and phase $\Phi = 0$. As δ is further increased the phase adjusts to maintain locking. The solid (dashed) curve indicates stable (unstable) solutions ($A_2 = -3.4375$).

λ is moderate (see Fig. 4b), the Arnold tongues shift to the right, are wider, and are spaced further apart.

3.3 Changing the modulation amplitude

We may investigate the behavior of the fixed points as a function of the modulation amplitude δ keeping $\Omega = 2\pi m/T_f$ fixed. The bifurcation equation is given by

$$\delta \cos(\Phi) = \delta_{SN} \tag{20}$$

where δ_{SN} is defined by (18). For a given frequency and operating conditions, $\delta = \delta_{SN}$ represents the minimum value of the modulation amplitude above which locking occurs. Our discussion of (20) will assume that δ is increased through the left boundary of the Arnold tongue when $\Phi = 0$ and $\delta = \delta_{SN}$.

The boundaries of the Arnold tongues in Figure 4 indicate δ_{SN} as a function of Ω. For $\delta < \delta_{SN}$, we expect a quasiperiodic behavior. For $\delta \geq \delta_{SN}$, we expect a periodic behavior as the phase Φ adjusts to maintain the desired frequency according to the bifurcation equation (20). Figure 5 shows the bifurcation from the left boundary of the Arnold tongue where $\Phi \in (-\pi/2, \pi/2)$ ($\Phi \in (\pi/2, 3\pi/2)$ on the right boundary). A linear stability analysis (see below) confirms that δ_{SN} is a saddle-node (SN) bifurcation point. We also find that as δ is further increased, a period doubling (PD) bifurcation is possible.

3.4 Linear stability of the fixed points

The linear stability of the fixed points is investigated by introducing the small perturbations t_n and d_n defined as

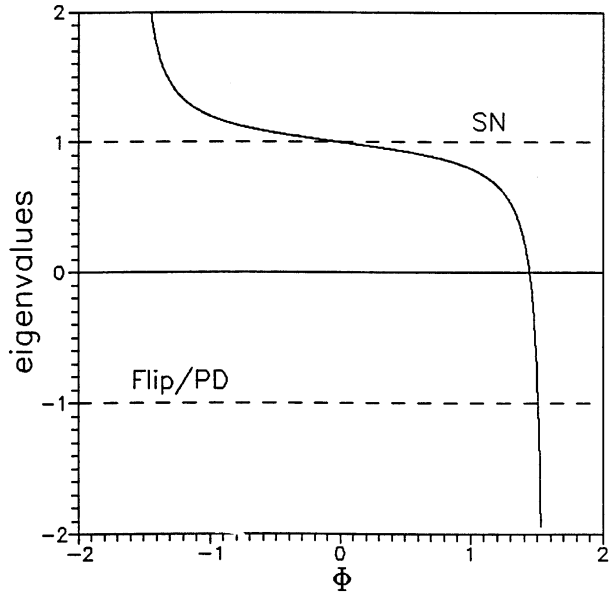

Fig. 6. Eigenvalues of linear-stability analysis for $\lambda = 0.1$, $T_\mathrm{f} = 50$ and $m = 1$ ($\Omega = 2\pi/T_\mathrm{f} = 0.1257$). The two eigenvalues are $r_1 = 0$ and r_2 given by (33).

$t_n \equiv T_n - (nT_\mathrm{f} + T_0)$ and $d_n \equiv D_n - D_\mathrm{f}$. The linearized problem for (t_n, d_n) has the form

$$t_{n+1} = m_{11} t_n + m_{12} d_n,$$
$$d_{n+1} = m_{21} t_n + m_{22} d_n \qquad (21)$$

where the coefficients m_{jk} are documented in the Appendix for A close to A_th. Again, we only discuss the left boundaries of the Arnold tongues, the discussion for the right boundaries being equivalent. Figure 6 gives the eigenvalues computed numerically. The figure shows that one eigenvalue is almost zero. We note that the second eigenvalue crosses 1 at $\Phi = 0$ with non-zero slope and therefore determines the SN bifurcation. The same eigenvalue crosses -1 when Φ is on the stable branch of node solutions, indicating a flip bifurcation. In the Appendix, we investigate this eigenvalue in detail in the case A close to A_th and show this flip bifurcation occur only for large amplitude of the modulations.

4 Discussion

By constructing a map based on the pulsating nature of PQS, we have analyzed the effect of periodic modulation. In particular, we have determined analytical conditions for the frequency-locking regimes, identified several Arnold tongues, and analyzed their linear stability properties. Outside the locking regions, the LMSA exhibits quasiperiodic solutions characterized by two frequencies, namely the frequency of the modulations and the detuning between the natural frequency of the laser and the frequency of the forcing. Quasiperiodic solutions correspond to non-fixed-point trajectories of the MPQS map. The properties of the frequency-locked (periodic) and unlocked (quasiperiodic) LMSA described by the MPQS-map have previously been observed in experiments and numerical simulations [12,18,19,22]; the MPQS-map provides useful formulas for how these behaviors depend on the parameters.

The equations of the map are valid provided the intensity is pulsating which is typically the case near the first laser threshold. Detailed comparisons between the solution of the full laser equations and the solution of the map have been done in the case of the free laser (see, for example, Fig. 3 in [23]) but have not been undertaken for the forced laser problem. Excellent agreement between these solutions has been observed in the free laser case provided that γ_1 and γ_2 are $O(10^{-3})$ or less which is the case for most LSAs. Noise has been ignored in all our analysis. Its effect is important and is documented in the literature (see, for example, [13,35]). If its amplitude is typically larger than $\exp(-1/\gamma_1)$, noise dramatically reduces the size of the pulsating oscillations. But the properties of these oscillations (maximum intensity and interpulse period) in terms of the fixed laser parameters are well described by the equations of the map.

In this paper we concentrated on the two-variable LMSA problem (3) when $\gamma_2 \gg \gamma_1$, which is valid for gas and solid-state lasers, including microchip lasers. For semiconductor lasers when $\gamma_2 \approx \gamma_1$ the analysis must start from equations (1). We have also derived the map appropriate for this case and found that the results are equivalent to those describe by the MPQS-map (8–11).

Of particular importance is the sensitivity of the LMSA if it is tuned close to threshold, *i.e.*, $A \approx A_\mathrm{th}$ such that the PQS output is high intensity and long period. In this regime, the Arnold tongues are very close together with respect to the forcing frequency; a slight change in the forcing frequency can cause locking to PQS of a different period. Also, the overlap of the tongues occurs for low forcing amplitude indicating the emergence of complex dynamical behavior.

The linear stability of high-intensity long-period PQS indicates that a PD bifurcation may occur if $\Phi \approx \pi/2$ which requires a very large forcing amplitude $\delta \gg 1$ (for fixed forcing frequency $\delta\cos(\Phi) = \delta_\mathrm{SN}$). It is easy to tune the parameters such that overlap with one of the other locking regions occurs before the PD bifurcation is reached; in this case quasiperiodic and other complex behavior may be exhibited instead of the usual period-doubling sequence to chaos. This is exactly what has been observed experimentally for modulated CO_2 lasers with a saturable absorber [36]. Finally, for $\delta = O(1)$ before any of these instabilities are reached, the linear-stability analysis shows that the LMSA is weakly stable with the eigenvalue for the map very close to one. Thus, in the pulsating regime close to A_th, the LMSA is likely to be sensitive to noise or other perturbations in its locked regime.

The well-known "circle map" [26] given by

$$\theta_{n+1} = \theta_n + \Omega + \frac{K}{2\pi}\sin(2\pi\theta_n), \qquad (22)$$

is the simplest map that characterizes a system exhibiting both periodic orbits and quasiperiodicity [26]. However,

Dangoisse *et al.* [19] have noted that the circle map does not capture all of the observed dynamics in experiments with LMSA. The MPQS-map (8–11) is specific for the LMSA and can be reduced to the Circle map as a special case. For large period orbits $P \gg 1$ ($\Omega \ll 1$), D_n is numerically small (D_n is the minimum value). Assume also the solution is nearly periodic so that $T_n \approx (2\pi m/\Omega)n$. Then from (10), we find

$$P \approx \frac{A}{A - A_{\rm th}}(1 + \delta\cos(\omega T_n + \Phi))$$

from which we obtain the circle map as

$$T_{n+1} = T_n + \frac{A}{A - A_{\rm th}}[1 + \delta\cos(\Omega T_n + \Phi)], \qquad (23)$$

with winding number proportional to $A/(A - A_{\rm th})$. As $A \to A_{\rm th}$ the period becomes infinite as expected near the homoclinic orbit.

T.W.C. is supported by National Science Foundation Grant No. DMS-9803207. The research by T.E. was supported by the US Air Force Office of Scientific Research grant AFOSR F49620-98-1-0400, the National Science Foundation grant DMS-9973203, the Fonds National de la Recherche Scientifique (Belgium) and the InterUniversity Attraction Pole program of the Belgian government.

Appendix: Linear stability of the fixed points

The linearized problem (21) exhibits complicated coefficients which we shall not detail. The analysis of the linearized problem is however much simpler if we consider $\lambda = A - A_{\rm th}$ small which is the domain of interest for strongly pulsating PQS regimes. Specifically, we assume the scaling

$$T_{\rm f} = O(\Omega^{-1}),\ \lambda = O(\Omega) \qquad (24)$$

as $\Omega \to 0$. The equations for the map are given by (8) and (9) where P and G satisfy equations (10, 11). Neglecting the $\exp(-T_{\rm f})$ small terms, these equations simplify as

$$\begin{bmatrix} \lambda P + D_n - A(1 + R\cos(\Omega T_n + \phi)) \\ +\frac{AR}{\Omega}[\sin(\Omega(T_n + P) + \phi) - \sin(\Omega T_n + \phi)] \end{bmatrix} \simeq 0, \quad (25)$$

and

$$G \simeq A[1 + R\cos(\Omega(T_n + P) + \phi)]. \qquad (26)$$

The fixed points solutions are given by equations (16–18) which simplifies as

$$R\cos(\Phi) = -1 + \frac{\lambda T_{\rm f}}{A_{\rm th}}\frac{\exp(\lambda T_{\rm f})}{\exp(\lambda T_{\rm f}) - 1}\,. \qquad (27)$$

The linearized problem for the deviations $t_n \equiv T_n - (nT_{\rm f} + T_0)$ and $d_n \equiv D_n - D_{\rm f}$ is now given by

$$\begin{aligned} t_{n+1} &= (1 + P_T)t_n + P_D d_n, \\ d_{n+1} &= \alpha\,[G_T t_n + G_D d_n] \end{aligned} \qquad (28)$$

where P_T, P_D, G_T, G_D denote partial derivatives of P and G with respect to T_n or D_n. They are defined by

$$\begin{aligned} P_T &= -\frac{A_{\rm th}R\Omega\sin(\Phi)}{\lambda + A_{\rm th}R\cos(\Phi)}, \\ P_D &= -\frac{1}{\lambda + A_{\rm th}R\cos(\Phi)}, \\ G_T &= -A_{\rm th}R\Omega\sin(\Phi)(1 + P_T), \\ G_D &= -A_{\rm th}R\Omega\sin(\Phi)P_D. \end{aligned} \qquad (29)$$

α is a function of $T_{\rm f}$ given by

$$\alpha = \frac{\exp(\lambda T_{\rm f}) - 1 - \lambda T_{\rm f}\exp(\lambda T_{\rm f})}{\exp(\lambda T_{\rm f})\,[\exp(\lambda T_{\rm f}) - 1 - \lambda T_{\rm f}]}\,. \qquad (30)$$

The solution of equation (28) is of the form $t_n = pr^n$ and $d_n = qr^n$ and r satisfies the following characteristic equation

$$r^2 - r(1 + P_T + \alpha G_D) = 0 \qquad (31)$$

which admit the solutions

$$\begin{aligned} r_1 &= 0, \\ r_2 &= 1 + P_T + \alpha G_D. \end{aligned} \qquad (32)$$

Using equations (29, 30), the second root can be rewritten as

$$r_2 = 1 - \Omega\tan(\Phi)\frac{[1 - \exp(\lambda T_{\rm f})]^2}{\exp(\lambda T_{\rm f})\,[\exp(\lambda T_{\rm f}) - 1 - \lambda T_{\rm f}]}\,. \qquad (33)$$

r_2 is clearly equal to 1 if $\Phi = 0$ where the SN bifurcation point is located. A flip or period doubling bifurcation is possible if $r_2 = -1$. However, because the second term in (33) is proportional to Ω, the bifurcation is only possible if Φ is close to $\pi/2$, meaning large R (large modulation amplitude δ). Introducing $\Phi = \pi/2 + \Omega\Phi_1$ into equation (33) with $r_2 = -1$ and simplifying leads to a critical value of Φ_1.

References

1. A.E. Siegman, *Lasers* (Univ. Science Books, 1986), p. 1024.
2. C.O. Weiss, R. Vilaseca, *Dynamics of Lasers* (VCH Weinheim, FRG, 1991).
3. Y.I. Khanin, *Principles of Laser Dynamics* (Elsevier, Amsterdam, 1995).
4. P. Mandel, *Theoretical Problems in Cavity Nonlinear Optics* (Camb. Stud. in Modern Optics, Camb. University Press, 1997).
5. E. Arimondo, F. Casagrande, L.A. Lugiato, P. Glorieux, Appl. Phys. B **30**, 5 (1983); E. Arimondo, P. Bootz, P. Glorieux, E. Menchi, J. Opt. Soc. Am. B **2**, 193 (1985).
6. M. Tachikawa, K. Tanii, T. Shimizu, J. Opt. Soc. Am. B **4**, 387 (1987); J. Opt. Soc. Am. B **5**, 1077 (1988).
7. J.J. Zayhowski, Opt. Lett. **21**, 588 (1996); *Errata*, Opt. Lett. **21**, 1618 (1996); J.J. Zayhowski, C. Dill III, Opt. Lett. **19**, 1427 (1994).

8. G.J. Spühler, R. Paschotta, R. Fluck, B. Braun, M. Moser, G. Zhang, E. Gini, U. Keller, J. Opt. Soc. Am. B **16**, 376 (1999).
9. G.P. Agrawal, N.K. Dutta, *Long-wavelength Semiconductor Lasers* (Van Nostrand Reinhold, New York, 1986).
10. H. Kawaguchi, *Bistabilities and Nonlinearities in Laser Diodes* (Artech House, Boston, 1994).
11. M. Yamada, IEEE J. Quant. Electr. **29**, 1330 (1993).
12. C. Juang, M.R. Chen, J. Juang, Opt. Lett. **24**, 1346 (1999).
13. C.R. Mirasso, G.H.M. van Tartwijk, E. Hernández-Garcia, D. Lenstra, S. Lynch, P. Landais, P. Phelan, J. O'Gorman, M. San Miguel, W. Elsässer, IEEE J. Quant. Electr. **35**, 764 (1999).
14. G.H.M. van Tartwijk, M. San Miguel, IEEE J. Quant. Electr. **32**, 1191 (1996).
15. I. Kidoguchi, H. Adachi, S. Kamiyama, T. Fukuhisa, M. Mannoh, A. Takamori, IEEE J. Quant. Electr. **33**, 831 (1997).
16. H.D. Summers, P. Rees, Appl. Phys. Lett. **71**, 2665 (1997).
17. D.R. Jones, P. Rees, I. Pierce, H.D. Summers, IEEE J. Select. Top. Quant. Electr. **5**, 740 (1999).
18. H.G. Winful, Y.C. Chen, J.M. Liu, Appl. Phys. Lett. **48**, 616 (1988).
19. D. Dangoisse, P. Glorieux, D. Hennequin, Phys. Rev. A **45**, 1551 (1990).
20. A. Egan, M. Harley-Stead, P. Rees, S. Lynch, J. O'Gorman, J. Egarty, IEEE Photon. Tech. Lett. **8**, 758 (1996).
21. A. Egan, J. O'Gorman, P. Rees, G. Farrell, J. Hegarty, P. Phelan, Electr. Lett. **31**, 808 (1996).
22. W. Lauterborn, I. Eick, J. Opt. Soc. Am. B **5**, 1089 (1988).
23. T. Erneux, P. Peterson, A. Gavrielides, Eur. Phys. J. D **10**, 423 (2000).
24. T.W. Carr, T. Erneux, to appear in the IEEE J. Quant. Electr. (in press, 2001).
25. H.T. Powell, G.J. Wolga, IEEE J. Quant. Electr. **7**, 213 (1971)
26. A.J. Lichtenberg, M.A. Lieberman, *Regular and Chaotic Dynamics*, 2nd edn. (Spinger-Verlag, New York, 1992).
27. S. Wiggins, *Introduction to Applied Nonlinear Dynamics* (Springer-Verlag, New York, 1990).
28. J. Kevorkian, J.D. Cole, *Multiple Scale and Singular Perturbation Methods* (Springer-Verlag, New-York, 1996).
29. T. Erneux, J. Opt. Soc. Am. B **5**, 1063 (1988).
30. P. Peterson, A. Gavrielides, M.P. Sharma, T. Erneux, IEEE J. Quant. Electr. **35**, 1247 (1999).
31. I.B. Schwartz, T. Erneux, SIAM J. Appl. Math. **54**, 1083 (1994).
32. T.W. Carr, L. Billings, I.B. Schwartz, I. Triandaf, Physica D **147**, 59 (2000).
33. R. Adler, Proc. IRE **34**, 351 (1946); reprinted in Proc. IEEE **61**, 1380 (1973).
34. S.H. Strogatz, *Nonlinear Dynamics and Chaos* (Addison Wesley, 1995).
35. M. Georgiou, T. Erneux, Phys. Rev. A **45**, 6636 (1992).
36. E. Arimondo, P. Glorieux, unpublished results, 1983.